Age-of-Information Minimization for UAV-Based Multi-View Sensing and Communication

Wenwen Jiang ⓘ, *Graduate Student Member, IEEE*, Bo Ai ⓘ, *Fellow, IEEE*, Chao Shen ⓘ, *Member, IEEE*, Mushu Li ⓘ, *Member, IEEE*, and Xuemin Shen ⓘ, *Fellow, IEEE*

Abstract—Due to flexible deployment and controllable mobility, unmanned aerial vehicles (UAVs) have great potential for supporting many time-critical sensing applications. In this article, we investigate UAV-based wireless sensing and communication in which one UAV with an onboard camera sensor senses ground targets from multiple different views and transmits the sensing data to a remote ground controller (GC). With the objective of improving the freshness of the information received at the GC while ensuring the sensing quality, we develop a *MUlti-view SensIng and Communication (MUSIC)* framework and jointly optimize the parameters in the framework including the target visiting sequence, the number of sensing, UAV trajectory, service time and transmit power. To solve the corresponding mixed-integer non-convex problem, we propose a two-stage approach. Specifically, we first determine the target visiting sequence by considering a specific case, i.e., UAV senses each target only once, through the quadratic penalty (QP) and successive convex approximation (SCA) methods. Based on the obtained visiting sequence, we minimize the average peak age-of-information (PAoI) of all targets by jointly optimizing the variables contained in the *MUSIC* framework via the SCA and exhaustion methods. Simulation results demonstrate that the proposed joint optimization approach outperforms the benchmark schemes.

Index Terms—Unmanned aerial vehicle (UAV), peak age-of-information (PAoI), multi-view sensing and communication (MUSIC), joint optimization.

I. INTRODUCTION

WITH the advance of the wireless networks, the applications of unmanned aerial vehicles (UAVs) [1] have been widely applied in military, public, and civil areas [2], [3]. UAVs can be deployed as wireless communication platforms to conduct critical tasks related to information collection [4], which has drawn significant research interest. However, it is challenging to collect fresh information in mission-critical scenarios [5] where no monitoring device is deployed due to the budgetary constraints, logistical challenges, adverse environmental conditions, etc. To solve the issue, UAVs can be equipped with sensing and communication modules to perform sensing tasks in many time-critical scenarios [6], such as road traffic monitoring [7], [8], forest fire surveillance [9], disaster monitoring [10], precision agriculture [11], and industrial facility inspection [12], [13]. Among these applications, UAVs can sense the information of interest from targets and transmit the sensed results to a ground controller (GC) for environmental analysis, scene reconstruction, life rescue, channel modeling, etc. Compared with in situ observation and conventional spaceborne and airborne remote sensing, UAV-based sensing and communication can collect high-resolution spatiotemporal information and conduct operations with high mobility and low operational cost in inaccessible areas [5]. Furthermore, the freshness of information depends on the timeliness of the sensed results during sensing and transmission, which has a critical impact on GC processing or decision-making. Due to dynamic changes in target status or environment, outdated information may lead to the wrong decisions at the GC. Thus, UAVs are required to frequently sense target information and transmit it to the GC in a timely and reliable manner to improve the freshness of the sensed information.

Age-of-information (AoI) [14] is an emerging performance metric to quantify the freshness of information. AoI is defined as the time elapsed since the most recent data update was generated, which is initially used in the Internet of Things (IoT) applications involving remote monitoring [15]. Peak AoI (PAoI) [16] is defined as the maximum value of the AoI before a new update is received. As shown in Fig. 1, the $(n-1)$-th update of a target is generated at the time instant t_{n-1}, the AoI a_n evolves over time since t_{n-1} until the n-th update received by the receiver at the time instant t'_n, a_n reaches its peak value, i.e., A_n. The lower the AoI is, the more fresh the information will be [17]. To keep the overall information received at the GC as fresh as possible,
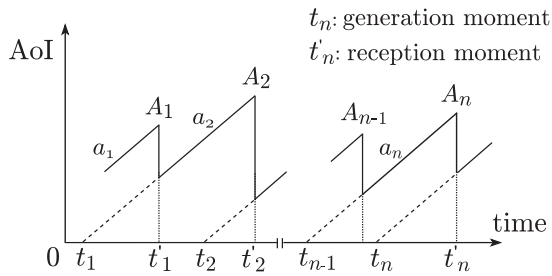
Fig. 1. Example of AoI evolution.

we adopt the average PAoI as a performance indicator in this article. The AoI accumulates from the end of the last sensing of the UAV until it peaks when the GC successfully receives an update of new sensing data.

In UAV-based sensing and communication, it is not straightforward to improve the information freshness by ensuring reliable sensing and communication. The UAV trajectory, target visiting sequence, and resource allocation are the key factors that determine the AoI of the sensing data. Due to the coupling relationships between these factors, it is challenging to minimize the AoI-related metrics while satisfying the stringent requirements of sensing quality and communication quality. Specifically, first, the sensing quality, which is limited by the sensing range of the onboard sensor, is determined by the sensing positions and the number of sensing, which should be considered in the UAV trajectory design. Second, the communication quality is determined by the UAV trajectory and the allocation of the communication resources, including transmit power and time. In addition, the UAV trajectory design is also affected by the target visiting sequence. Consequently, an efficient joint optimization approach needs to be well-developed to support UAV-based sensing and communication for improving information freshness.

In this article, we investigate a UAV-based wireless sensing and communication system, in which one UAV performs sensing for each target from multiple different views sequentially and then transmits the sensing data to the GC. The objective of the paper is to minimize the average PAoI of all sensing data and the main contributions are summarized as follows:

- We develop a *MUlti-view SensIng and Communication (MUSIC)* framework for the UAV-based wireless sensing and communication system to improve the sensing success probability, sensing precision influenced by the sensing views, and communication reliability. Based on the framework, we formulate an average PAoI minimization problem by jointly optimizing the target visiting sequence, the total number of sensing, transmit power, UAV trajectory, and the time allocation during sensing, flying, and transmission.
- We propose a two-stage approach to solve the formulated mixed-integer non-convex problem. Specifically, in the first stage, we solve the average PAoI minimization problem with $S = 1$ to obtain an efficient target visiting sequence based on the quadratic penalty (QP) [18] and the successive convex approximation (SCA) [19] methods. In the second stage, based on the obtained target visiting sequence, we optimize the average PAoI minimization

problem with $S > 1$ by jointly optimizing the optimization variables contained in the *MUSIC* framework through the SCA and exhaustive methods.
- Simulation results demonstrate the effectiveness of the developed *MUSIC* framework, which can guarantee the freshness of sensed information and the requirements of sensing and communication quality. The optimized target visiting sequence is verified to outperform the nearest neighbor visiting policy and random visiting policy. Meanwhile, the proposed joint optimization algorithm performs better than the alternating optimization (AO) algorithm [20] in improving the information freshness.

The remainder of this article is organized as follows. Related work is presented in Section II. The system model is introduced in Section III. In Section IV, an average PAoI minimization problem is formulated. In Section V, an iterative algorithm is designed based on QP and SCA methods for determining an efficient target visiting sequence. Then, an algorithm based on SCA and exhaustive methods is developed to solve the average PAoI minimization problem in Section VI. Simulation results and performance analysis are shown in Section VII. Finally, we conclude this article in Section VIII.

Notations: In this article, scalars, column vectors, and matrices are written in italic, boldfaced lower-case, and upper-case letters, respectively, e.g., x, $\mathbf{x}$, and $\mathbf{X}$. The superscript $(\cdot)^T$ indicates the transpose. The operator $\| \mathbf{x} \|_2$ represents the Euclidean norm of vector $\mathbf{x}$. In addition, the space of K-dimensional real-valued vector is denoted by $\mathbb{R}^K$. The set of integers is denoted by $\mathbb{Z}$. The logarithm with base 2 is denoted by $\log_2(\cdot)$. Given set $\mathcal{N} \triangleq \{1, \ldots, N\}$, $\bar{\mathcal{N}} \triangleq \mathcal{N} \setminus \{N\}$ represents the set of elements in $\mathcal{N}$ other than N.

II. RELATED WORK

Among the existing research work related to UAVs [1], [2], [3], [4], [5], [6], most studies focusing on trajectory design and resource allocation for UAV-based sensing [8], [9], [10], [11], [12] or UAV-based communication [21], [22], [23], [24], [25], [26], [27], [28], [29] individually. Recently, there are also some research contributions focusing on UAV-based sensing and communication out of the considerations of the UAV endurance [30], energy efficiency [31], and information freshness [32], [33], [34]. In this section, we mainly focus on summarizing related studies on UAV-based communication and UAV-based sensing and communication under different concerns.

A. UAV-Based Communications

There are many research efforts focusing on trajectory design and resource allocation from the perspective of UAV endurance or energy efficiency. Gong et al. [21] aimed to minimize the UAV total flight time while allowing each sensor to successfully upload a certain amount of data using limited energy by jointly optimizing the data collection intervals, UAV speed and the sensors' transmit powers. Zhan and Zeng [22] aimed to minimize the maximum mission completion time among all UAVs by jointly optimizing the UAV trajectory, wake-up scheduling, and association for sensor nodes while ensuring that
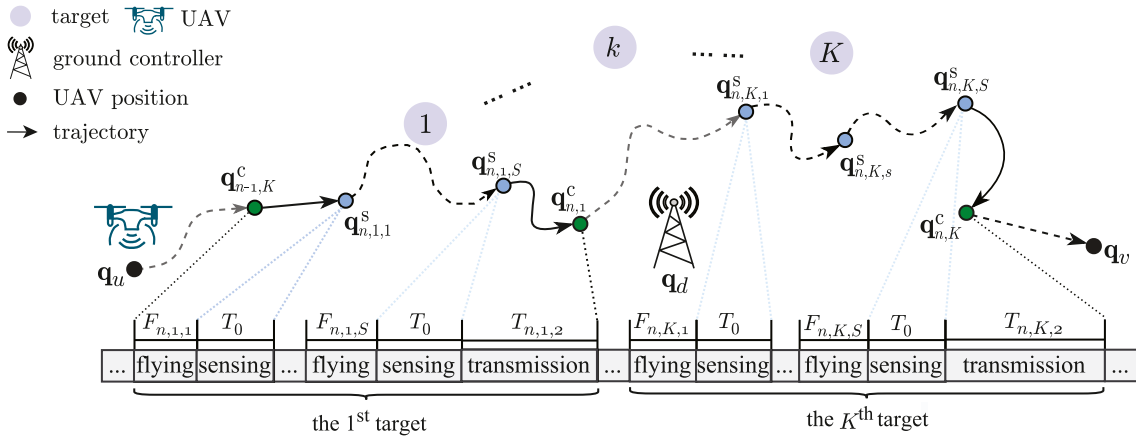
Fig. 2. System model with K targets, one ground controller (GC), and one UAV in the n-th update cycle (*MUSIC* Framework).

each SN can successfully upload the targeting amount of data with a given energy budget. Zhang et al. [23] investigated an energy-saving UAVs deployment problem, and they proposed a heuristic energy-saving algorithm by jointly balancing heterogeneous UAVs' flying distances on the ground and final service altitudes in the sky. Ding et al. [24] studied a 3D UAV trajectory design and band allocation problem considering both the energy consumption of the UAV and the fairness among the ground users. Li et al. [25] aimed to maximize the energy efficiency of the UAV by jointly optimizing the UAV trajectory, the user transmit power, and computation load allocation in a UAV-assisted mobile edge computing system. Wang et al. [26] studied how to dynamically design the path planning for cooperative UAV-swarm while satisfying the spatio-temporally demands of users. In addition, there is also some research on UAV-based communication aimed at optimizing AoI by jointly optimizing the trajectory design and resource allocations [27], [28], [29].

B. UAV-Based Sensing and Communication

Sensing and communication is an interesting research topic, which has been investigated in many studies recently [35], [36]. Among these studies, there are a few studies focusing on UAV-based sensing and communication. Liu et al. [30] investigated a UAV-based environmental monitoring system, wherein a UAV trajectory planning problem is formulated to minimize the UAV mission completion time by jointly optimizing the flying speeds, hovering positions, and visiting sequence while considering the AoI of data and the UAV onboard energy. In [31], Zhang et al. studied the UAV energy efficiency maximization problem by optimizing the UAV sensing and transmission in a cellular UAV system. There are also some studies taking AoI-related metrics as the optimization objectives [32], [33], [34]. In [32], the authors considered an AoI minimization problem in the cellular internet of UAVs by jointly optimizing the service time, UAV trajectory, and task scheduling. To achieve a higher successful sensing probability, each UAV is required to sense its task multiple times, and the sensing position for a task remains the same. Hu et al. [33] considered a case where the UAV performs each target once sensing within its maximum sensing range, they proposed a

distributed sense-then-send protocol and formulated a trajectory design problem for AoI minimization. In [34], Wu et al. designed a joint sensing and transmission protocol and investigated an AoI minimization problem by designing trajectories in the UAV cellular network, where the UAV performs each target once sensing. All of these works inspire us to investigate AoI optimization in UAV-based wireless sensing and communication systems with requirements of sensing quality and reliable communication.

III. SYSTEM MODEL

We consider a UAV-based wireless sensing[1] and communication scenario, as shown in Fig. 2, wherein there are K targets of interest, one UAV, and one GC. Since the targets are far away from the GC, one UAV with sensing and communicating capabilities is deployed to sense information of interest from targets and transmit the sensed results to the remote GC for further processing. Specifically, the UAV fly over the targets to sense their information successively. Whenever the UAV completes the sensing for a target, the UAV transmits the sensed information to the GC through the onboard communication module immediately. The positions of targets are known in advance.[2] Denote the position of the k-th target by $\mathbf{q}_k \in \mathbb{R}^2, \forall k \in \mathcal{K} \triangleq \{1, \ldots, K\}$. Without loss of generality, the UAV flight altitude is fixed at h meters.

Note that the sensing is not always successful due to the physical limitations of the onboard sensor and possible uncontrollable accidents in practice. The probabilistic sensing model [30], [31], [32], [33], [34], [37] is adopted in this article to evaluate the sensing success probability, and the probability can be improved by increasing the number of sensing [32]. Different sensing positions have different sensing views to a target. Multiple different sensing views can increase the diversity of the sensing information related to a target and allow the UAV

---

[1]To perform sensing, the UAV can carry the onboard sensor modules (e.g., the specialized optical and thermal sensor, the visual imagery sensor, and the infrared sensor camera), which can detect information about the target. The information can be fire-related events, road traffic information, and post-disaster signs of life for rescue, etc.

[2]The number and positions of targets to be sensed can be determined by the previous experience of events of interest or by existing satellite remote sensing techniques in the planning phase before the system operation.

to detect the information that is blocked by obstacles in a single view. Therefore, to improve the sensing quality, we propose a *MUlti-view SensIng and Communication (MUSIC)* framework which is described as follows: (1) The UAV departs from the starting position $\mathbf{q}_u \in \mathbb{R}^2$ and moves toward the first target to be visited. (2) The UAV selects a suitable sensing position within the sensing range to sense data from the target for T_0 seconds. The sensing position remains unchanged during the sensing for ensuring stability and quality. (3) Subsequently, the UAV moves to a new sensing position and senses the target information from a new view. The duration of each sensing remains constant. (4) After the UAV performs S sensings from different views, all sensing results are aggregated into one packet and forwarded to the GC denoted by $\mathbf{q}_d \in \mathbb{R}^2$. (5) At last, the UAV moves toward the next target to be visited. Steps (2)–(4) are repeated until tasks for all targets are completed. At last, the UAV returns to the final position $\mathbf{q}_v \in \mathbb{R}^2$. The process by which the UAV completes S sensing and once transmission for K targets is defined as an update cycle. A total of N update cycles are considered in this scenario.

A. Visiting Sequence Model

Each target has an initial label, denoted by $m \in \mathcal{K}$. The target visiting sequence is denoted by $k \in \mathcal{K}$, with the sequence mapping by π, i.e., $k = \pi(m), \forall m \in \mathcal{K}$. We introduce a binary matrix, $\mathbf{x}$, to represent the target visiting sequence, where element $x_{m,k} \in \{0,1\}$ indicates whether the target with label m is visited for the k-th time. Specifically, $x_{m,k} = 1$ if the k-th target visited by the UAV is the target with label m; otherwise, $x_{m,k} = 0$. Therefore, the order of the target m visited by the UAV is given by $k = \pi(m) = \sum_{i=1}^{K} i x_{m,i}$, and the position of the k-th visiting target is denoted by $\mathbf{s}_k = \mathbf{W}\mathbf{x}_k, \forall k$, where $\mathbf{W} = [\mathbf{q}_1, \ldots, \mathbf{q}_m, \ldots, \mathbf{q}_K] \in \mathbb{R}^{2 \times K}$ and $\mathbf{x}_k = [x_{1,k}, \ldots, x_{m,k}, \ldots, x_{K,k}]^T \in \{0,1\}^K, \forall k$. The optimization of the visiting policy π is to optimize $\{x_{m,k}, \forall m, k\}$. We assume that the UAV can sense only one target at a time, and each target is served only once in each update cycle, i.e.,

$$x_{m,k} \in \{0,1\}, \sum_{m=1}^{K} x_{m,k} = 1, \sum_{k=1}^{K} x_{m,k} = 1, \forall m, k \in \mathcal{K}. \quad (1)$$

B. UAV Trajectory Model

The UAV trajectory can be approximated by a series of positions among time segments. For the k-th target in the n-th update cycle, we denote by $\mathbf{q}_{n,k,s}^{\mathrm{s}} \in \mathbb{R}^2$ the s-th sensing position of the UAV and $\mathbf{q}_{n,k}^{\mathrm{c}} \in \mathbb{R}^2$ the packet transmission end position. As illustrated in Fig. 2, the flight time between the sensing positions $\mathbf{q}_{n,k,s-1}^{\mathrm{s}}$ and $\mathbf{q}_{n,k,s}^{\mathrm{s}}$ is defined as $F_{n,k,s}$. Each sensing lasts for T_0 seconds. The service time for the k-th target in the n-th update cycle, denoted by $T_{n,k}$, which is mathematically expressed as

$$T_{n,k} = T_{n,k,1} + T_{n,k,2},$$

$$= \sum_{s=1}^{S} (F_{n,k,s} + T_0) + T_{n,k,2}, \forall n \in \mathcal{N}, k \in \mathcal{K}, \quad (2)$$

where $T_{n,k,1}$ is the sum of the multiple flight time $F_{n,k,s}$ and sensing duration T_0, and $T_{n,k,2}$ is the packet transmission time from the UAV to the GC. $S \in \mathbb{Z}$ represents the total number of sensing for a target in each update cycle. Superscripts s and c are signs of the sensing position and communication position, respectively. Subscripts $n, k, s, 1$, and 2 represent the n-th update cycle, the k-th target, the s-th sensing, the sensing phase, and communication phase, respectively. Then, the total service time of the n-th update cycle is given by

$$T_n = \sum_{k=1}^{K} \left(\sum_{s=1}^{S} (F_{n,k,s} + T_0) + T_{n,k,2} \right), \forall n \in \mathcal{N}. \quad (3)$$

The distance constraints over consecutive positions due to the flight speed limit are modeled by

$$\|\mathbf{q}_{1,1,1}^{\mathrm{s}} - \mathbf{q}_u\|_2 \leq v_{\max} F_{1,1,1}, \quad (4a)$$

$$\|\mathbf{q}_{n,k,s}^{\mathrm{s}} - \mathbf{q}_{n,k,s+1}^{\mathrm{s}}\|_2 \leq v_{\max} F_{n,k,s+1}, \forall n \in \mathcal{N},$$
$$k \in \mathcal{K}, s \in \bar{\mathcal{S}} \triangleq \mathcal{S} \setminus \{S\}, \quad (4b)$$

$$\|\mathbf{q}_{n,k,S}^{\mathrm{s}} - \mathbf{q}_{n,k}^{\mathrm{c}}\|_2 \leq v_{\max} T_{n,k,2}, \forall n \in \mathcal{N}, k \in \mathcal{K}, \quad (4c)$$

$$\|\mathbf{q}_{n,k}^{\mathrm{c}} - \mathbf{q}_{n,k+1,1}^{\mathrm{s}}\|_2 \leq v_{\max} F_{n,k+1,1}, \forall n \in \mathcal{N}, k \in \bar{\mathcal{K}}, \quad (4d)$$

$$\|\mathbf{q}_{n,K}^{\mathrm{c}} - \mathbf{q}_{n+1,1,1}^{\mathrm{s}}\|_2 \leq v_{\max} F_{n+1,1,1}, n \in \bar{\mathcal{N}}, \quad (4e)$$

$$\|\mathbf{q}_{N,K}^{\mathrm{c}} - \mathbf{q}_v\|_2 \leq v_{\max}(T_{\max} - U_N - T_N), \quad (4f)$$

where $\mathcal{S} \triangleq \{1, \ldots, S\}$, $\bar{\mathcal{K}} \triangleq \mathcal{K} \setminus \{K\}$. $v_{\max}$ is the maximum flight speed of the UAV. $T_{\max}$ is the maximum endurance of the UAV which is large enough for the UAV to complete the tasks among N update cycles. Constraint (4a) represents the maximum distance constraint between the starting position $\mathbf{q}_u$ and the first sensing position $\mathbf{q}_{1,1,1}^{\mathrm{s}}$. Constraints (4b), (4d), and (4e) are the maximum distance constraints between adjacent sensing positions, adjacent targets, and adjacent update cycles, respectively. Constraint (4c) indicates the maximum distance constraint in the transmission phase. Constraint (4f) requires that the UAV returns to the final position $\mathbf{q}_v$ when all missions are completed.

C. Multi-View Probabilistic Sensing Model

The sensing quality[3] is critical to the decision-making of the GC. The UAV may fail to capture the key information due to the limited sensing range and the sensing precision [38]. Therefore, we use a probabilistic sensing model [30], [31], [32], [33], [34] to characterize the sensing success probability. The sensing success probability for each target can be improved by sensing the target multiple times [32]. However, since the sensing model fails to characterize the impact of information diversity, we further propose a multi-view sensing model.

1) Probabilistic Sensing Model: The sensing success event is a random variable, and its probability is negatively correlated with the sensing distance. To evaluate the sensing quality, the

---

[3]The UAV in this article has no computing capability and cannot immediately judge whether the sensing is successful. Thus, the sensing data needs to be sent to the GC for further processing to verify the validity of the sensed information. The sensing quality refers to the sensing success probability.

sensing success probability for the s-th sensing of the k-th target in the n-th update cycle is modeled by

$$p_{n,k,s} = \begin{cases} e^{-\mu d_{n,k,s}}, & \text{if } d_{n,k,s} \sin \phi \leq r, \\ 0, & \text{otherwise,} \end{cases} \quad (5)$$

for all $n \in \mathcal{N}, k \in \mathcal{K}, s \in \mathcal{S}$, where r is the maximum sensing range limit, $\mu > 0$ is a sensing factor representing the sensor sensitivity [37], $d_{n,k,s} = \sqrt{\|\mathbf{q}_{n,k,s}^{\mathrm{s}} - \mathbf{W}\mathbf{x}_k\|_2^2 + h^2}$ is the distance between the UAV at the s-th sensing position $\mathbf{q}_{n,k,s}^{\mathrm{s}}$ and the position of the k-th target to be visited $\mathbf{W}\mathbf{x}_k$, and ϕ is a maximum sensing angle of the onboard sensor. Therefore, the target is required to be within the sensing range of the onboard sensor, where

$$\|\mathbf{q}_{n,k,s}^{\mathrm{s}} - \mathbf{W}\mathbf{x}_k\|_2 \leq r \triangleq h \tan \phi, \forall n \in \mathcal{N}, k \in \mathcal{K}, s \in \mathcal{S}. \quad (6)$$

2) Multi-View Sensing Model: We can improve the sensing success probability for each target by increasing the number of sensing. However, when the sensing views are similar, the sensing data is highly correlated. Multiple sensing cannot provide additional information. Equation (5) cannot reflect the impact of the diversity of the sensing data.

Given that the sensing view of the UAV has an impact on the sensing precision in some applications [8], [9], [10], [11], [12]. We define θ as the minimum view angle difference for ensuring that the sensing views are different. The value of θ is set according to the requirements of the specific use cases. To ensure the sensing success probability and improve the sensing precision, we develop a multi-view sensing model based on (5) in this article. The adjacent sensing positions relative to the target s_k should be larger than θ, i.e.,

$$\angle \left(\overrightarrow{s_k \mathbf{q}_{n,k,(s+1)}^{\mathrm{s}}}, \overrightarrow{s_k \mathbf{q}_{n,k,s}^{\mathrm{s}}} \right) \geq \theta, \forall n \in \mathcal{N}, k \in \mathcal{K}, s \in \bar{\mathcal{S}}, \quad (7)$$

where $\angle$ represents the angle between vectors $\overrightarrow{s_k \mathbf{q}_{n,k,(s+1)}^{\mathrm{s}}}$ and $\overrightarrow{s_k \mathbf{q}_{n,k,s}^{\mathrm{s}}}$. To ensure that (7) is satisfied, the minimum distance $d_{\min}$ between adjacent sensing positions is given by

$$\|\mathbf{q}_{n,k,s}^{\mathrm{s}} - \mathbf{q}_{n,k,s+1}^{\mathrm{s}}\|_2 \geq d_{\min}, \forall n \in \mathcal{N}, k \in \mathcal{K}, s \in \bar{\mathcal{S}}. \quad (8)$$

By geometric analysis, $d_{\min}$ which is determined by θ can be expressed as

$$d_{\min} = \max \left\{ h \tan \theta, r - h \tan(\phi - \theta), \right.$$

$$\left. \sqrt{(2 - 2\cos\theta)(h^2 + r^2)} \right\}. \quad (9)$$

Based on the above analysis, the overall sensing success probability for the k-th target in the n-th update cycle is given by

$$P_{n,k} = 1 - \prod_{s=1}^{S}(1 - e^{-\mu d_{n,k,s}}) \geq P_{\mathrm{th}}, \forall n \in \mathcal{N}, k \in \mathcal{K}, \quad (10)$$

where P_{th} is the minimum required threshold for the total sensing success probability.

D. AoI Evolution Model

The AoI in this article characterizes the evolution of the packet age over time from its generation to its reception at the GC. Recall that all results sensed by the UAV for each target will be aggregated into one packet and sent to the GC. Let the starting moment of the n-th update cycle be

$$U_n = \sum_{i=1}^{n-1} T_i = U_{n-1} + T_{n-1}, n = 2, \ldots, N, \quad (11)$$

and denote the starting moment of the service time $T_{n,k}$ for the k-th target in the n-th update cycle by

$$U_{n,k} = U_n + \sum_{j=1}^{k-1} T_{n,j}, \quad (12a)$$

$$= U_n + \sum_{j=1}^{k-1} \left(\sum_{s=1}^{S}(F_{n,j,s} + T_0) + T_{n,j,2} \right), \quad (12b)$$

for all $n \in \mathcal{N}, k \in \mathcal{K}$, where $U_1 = U_{1,1} = 0$.

As shown in Fig. 3, the AoI of the k-th target in the n-th update cycle increases over time, and it will reach a peak $a_{n,k}$ when the GC successfully receives the packet of the k-th target in the $(n+1)$-th update cycle. Thus, we can characterize the PAoI of the k-th target in the n-th update cycle as (13) shown at the bottom of this page, where the first term of (13b) is the sum of the service time from the k-th target to the K-th target in the n-th update cycle; the second term is the sum of the target service time from the first target to the k-th target in the $(n+1)$-th update cycle; and the third term is the sum of all flight time and sensing duration for the k-th target in the n-th update cycle.

In order to measure the overall performance of the system, the average PAoI of all packets sensed from all targets among all update cycles is given by

$$\mathrm{API} = \frac{1}{K(N-1)} \sum_{n=1}^{N-1} \sum_{k=1}^{K} a_{n,k}. \quad (14)$$

$$a_{n,k} = U_{n+1,k} + T_{n+1,k} - (U_{n,k+1} - T_{n,k,2}) = \sum_{j=k}^{K} T_{n,j} + \sum_{j=1}^{k} T_{n+1,j} - \sum_{s=1}^{S}(F_{n,k,s} + T_0), \quad (13a)$$

$$= \sum_{j=k}^{K} \left(\sum_{s=1}^{S}(F_{n,j,s} + T_0) + T_{n,j,2} \right) + \sum_{j=1}^{k} \left(\sum_{s=1}^{S}(F_{n+1,j,s} + T_0) + T_{n+1,j,2} \right) - \sum_{s=1}^{S}(F_{n,k,s} + T_0), \forall n \in \bar{\mathcal{N}}, k \in \mathcal{K} \quad (13b)$$
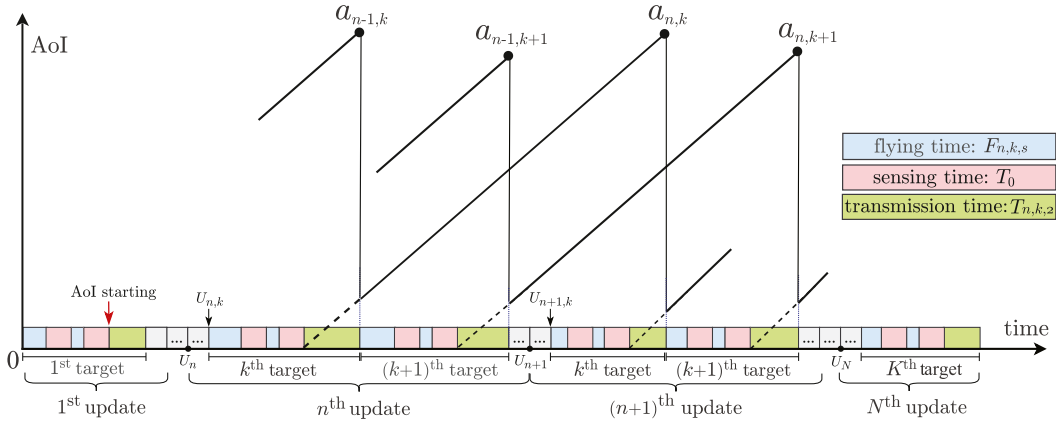
Fig. 3. Time discretization and AoI evolution with time (taking $S = 2$ as an example).

Minimizing the PAoI for each target can minimize the upper bound of the AoI, thus, the obtained optimization solution can provide a lower bound for the freshness performance. The design objective in this article is to minimize the average PAoI of all packets among N update cycles, which can raise the lower bound of the freshness performance.

E. Communication Model

According to the field measurement of the air-to-ground (A2G) channel, the line-of-sight (LOS) link dominates the A2G channels when the UAV altitude is sufficiently high [39]. Therefore, the channel power gain from the UAV located in $\mathbf{q}_{n,k}^{c}$ to the GC in the n-th update cycle can be modeled as

$$g_{n,k} = \frac{\mu_0}{h^2 + \|\mathbf{q}_{n,k}^{c} - \mathbf{q}_d\|_2^2}, \ \forall n \in \mathcal{N}, k \in \mathcal{K}, \quad (15)$$

where μ_0 is the reference channel gain at the distance of 1 m.

The Doppler effect due to the UAV mobility is assumed to be well compensated. According to the Shannon capacity, we approximate the achievable transmission rate $R_{n,k}$ for the communication bandwidth B by the instantaneous rate at the transmission end position $\mathbf{q}_{n,k}^{c}$, which is

$$R_{n,k} = BT_{n,k,2} \log_2 \left(1 + \frac{\gamma_0 p_{n,k}}{h^2 + \|\mathbf{q}_{n,k}^{c} - \mathbf{q}_d\|_2^2} \right), \quad (16)$$

for all $n \in \mathcal{N}, k \in \mathcal{K}$, where $\gamma_0 = \frac{\mu_0}{\Gamma\sigma^2}$. Γ indicates the signal-to-noise ratio (SNR) gap due to the practical modulation and coding scheme (MCS). σ^2 stands for the power of additive Gaussian white noise. $p_{n,k}$ is the UAV transmit power. The rate value obtained by (16) indicates the maximum transmission rate, which can be regarded as a theoretical performance upper bound of the practical transmission rate.[4]

Due to the limited radio frequency (RF) output power, the UAV has a maximum power limitation $P_{\max}$, i.e.,

$$0 \leq p_{n,k} \leq P_{\max}, \forall n \in \mathcal{N}, k \in \mathcal{K}. \quad (17)$$

[4]Although there is a gap between the transmission rate in theory and practice, it can provide an upper limit of transmission rate that can be approached through practical engineering design.

Based on the proposed *MUSIC* framework, we assume that the onboard sensor equipped on the UAV generates the sensing data at a fixed rate of R Mbit/s. Thus, the size of a packet carrying the sensing results for one target is expressed as $ST_0 R$. To ensure that the data sensed by the UAV for the target with label m can be reliably transmitted to the GC, the following condition should be satisfied

$$\sum_{k=1}^{K} x_{m,k} R_{n,k} \geq ST_0 R, \ \forall n \in \mathcal{N}, m \in \mathcal{K}. \quad (18)$$

IV. PROBLEM FORMULATION

The timeliness of the information sensed by the UAV is crucial for GC decision-making. To improve the freshness of the information contained in the data received at the GC, we formulate an average PAoI minimization problem for all targets among N update cycles subject to the sensing quality and reliable transmission requirements. To this end, we jointly optimize the target visiting sequence $\{x_{m,k}, \forall m, k\}$, number of sensing S, UAV trajectory $\{\mathbf{q}_{n,k,s}^{s}, \mathbf{q}_{n,k}^{c}, \forall n, k, s\}$, as well as service time $\{F_{n,k,s}, T_{n,k,2}, \forall n, k, s\}$ and transmit power $\{p_{n,k}, \forall n, k\}$.

To keep the freshness of the information received at the GC up-to-date, the optimization problem is formulated as follows

$$(\text{P}_1) \min_{\substack{\{x_{m,k}, p_{n,k}, S, F_{n,k,s}, \\ T_{n,k,2}, \mathbf{q}_{n,k,s}^{s}, \mathbf{q}_{n,k}^{c}\}}} \text{API}$$

$$\text{s.t. } (1), (4), (6), (8), (10), (17), (18). \quad (19)$$

Constraint (1) indicates the requirement of the visiting sequence. Constraint (4) is the set of the distance constraints due to $v_{\max}$. Constraint (6) is the sensing range limitation. Constraint (8) represents the minimum distance used for adjusting sensing views. Constraint (10) guarantees the sensing quality. Constraint (17) imposes a limit on the UAV transmit power. Constraint (18) ensures the reliable transmission.

Lemma 1: The optimal UAV transmit power $p_{n,k}^{*}$ is $P_{\max}$.

Proof: Note that the UAV transmit power in Problem (P_1) is determined by Constraints (17) and (18). When the number of sensing S is fixed, the packet size required to be transmitted is determined. Constraint (18) can be guaranteed by increasing the

values of $T_{n,k,2}$ and $p_{n,k}$. Given that the objective of Problem (P_1) is to minimize the average PAoI, which is a monotonically increasing function in $T_{n,k,2}$. In Constraint (18), the transmission time $T_{n,k,2}$ can be minimized only when the UAV transmit power is maximized, i.e., $p_{n,k} = P_{\max}$. Otherwise, the objective function obtained is not optimal and can be further reduced by increasing $p_{n,k}$. Thus, the optimum transmit power in Problem (P_1) is the maximum transmit power $P_{\max}$. This completes the proof. ∎

Given the optimum transmit power, i.e., $P_{\max}$, the challenges of solving Problem (P_1) mainly lie in two aspects. First, Constraints (1), (6), (10), and (18) involve integer variables $\{x_{m,k}\}$ and S, which makes Problem (P_1) a mixed-integer problem. Second, the coupling of optimization variables $\{S, T_{n,k,2}, \mathbf{q}^s_{n,k,s}, \mathbf{q}^c_{n,k}\}$ makes Constraints (10) and (18) non-convex. Constraint (8) is also non-convex. Problem (P_1) as an NP-hard problem that cannot be solved directly by off-the-shelf convex solvers.

To solve these challenges, we propose a two-stage approach to solve Problem (P_1) efficiently for obtaining a sub-optimal solution. Specifically, we first optimize Problem (P_1) by considering a specific case with $S = 1$ to simplify the problem-solving and determine the target visiting sequence. Since the sensing time is relatively small compared to the flight time of the UAV, the impact of changing the number of sensing S on optimizing the target visiting sequence can be negligible. Therefore, using the obtained target visiting sequence obtained in the first stage, we solve Problem (P_1) by jointly determining $\{S, F_{n,k,s}, T_{n,k,2}, \mathbf{q}^s_{n,k,s}, \mathbf{q}^c_{n,k}\}$ for minimizing the average PAoI in the second stage.

V. VISITING SEQUENCE OPTIMIZATION

To reduce the dimension of decision spaces in solving Problem (P_1), we first consider a specific case with $S = 1$ in the first stage to solve Problem (P_1) for determining the target visiting sequence.

A. Problem Formulation for Visiting Sequence

In this case, the service time $T_{n,k}$ of the k-th target in the n-th update cycle consists of three components

$$T_{n,k} = F_{n,k} + T_0 + T_{n,k,2}, \forall n \in \mathcal{N}, k \in \mathcal{K}, \quad (20)$$

where $F_{n,k}$, T_0 and $T_{n,k,2}$ are the time durations for flight, sensing and transmission, respectively. Based on (13), the PAoI $a_{n,k}$ when $S = 1$ is expressed as

$$a_{n,k} = \sum_{j=k}^{K} T_{n,j} + \sum_{j=1}^{k} T_{n+1,j} - F_{n,k} - T_0 \quad (21a)$$

$$= T_{n,k,2} + \sum_{j=k+1}^{K} (F_{n,j} + T_0 + T_{n,j,2})$$

$$+ \sum_{j=1}^{k} (F_{n+1,j} + T_0 + T_{n+1,j,2}), \forall n \in \bar{\mathcal{N}}, k \in \mathcal{K}. \quad (21b)$$

Therefore, the average PAoI when $S = 1$ can be characterized according to (14).

The distance constraints over consecutive positions due to the flight speed limit in (4) can be reduced to

$$\|\mathbf{q}^s_{1,1} - \mathbf{q}_u\|_2 \leq v_{\max} F_{1,1}, \quad (22a)$$

$$\|\mathbf{q}^c_{n,k} - \mathbf{q}^s_{n,k}\|_2 \leq v_{\max} T_{n,k,2}, \forall n \in \mathcal{N}, k \in \mathcal{K}, \quad (22b)$$

$$\|\mathbf{q}^s_{n,k+1} - \mathbf{q}^c_{n,k}\|_2 \leq v_{\max} F_{n,k+1}, \forall n \in \mathcal{N}, k \in \bar{\mathcal{K}}, \quad (22c)$$

$$\|\mathbf{q}^s_{n,K} - \mathbf{q}^c_{n+1,1}\|_2 \leq v_{\max} F_{n+1,1}, \forall n \in \bar{\mathcal{N}}, \quad (22d)$$

$$\|\mathbf{q}^c_{N,K} - \mathbf{q}_v\|_2 \leq v_{\max}(T_{\max} - U_N - T_N), \quad (22e)$$

where $\mathbf{q}^s_{n,k}$ and $F_{n,k}$ represent the sensing position and the flight time, respectively, for the k-th target in the n-th update cycle by dropping the subscript s for ease of notations.

The sensing distance constraint between the UAV and its k-th visiting target in (6) is simplified as

$$\|\mathbf{q}^s_{n,k} - \mathbf{W}\mathbf{x}_k\|_2 \leq r, \forall n \in \mathcal{N}, k \in \mathcal{K}. \quad (23)$$

The data transmission requirement for the target m is

$$\sum_{k=1}^{K} T_{n,k,2} \log_2 \left(1 + \frac{\gamma_0 P_{\max} x_{m,k}}{h^2 + \|\mathbf{q}^c_{n,k} - \mathbf{q}_d\|_2^2} \right) \geq \frac{T_0 R}{B}, \quad (24)$$

for all $n \in \mathcal{N}$, $m \in \mathcal{K}$. Therefore, the target visiting sequence determination problem can be formulated as

$$(P_2) \quad \min_{\{x_{m,k}, F_{n,k}, T_{n,k,2}, \mathbf{q}^s_{n,k}, \mathbf{q}^c_{n,k}\}} \text{API}$$

$$\text{s.t. } (1), (22), (23), (24). \quad (25)$$

Problem (P_2) is still a mixed-integer non-convex problem, but it can be transformed into a convex problem by relaxing $x_{m,k}$ into a continuous variable and dealing with the non-convex constraint (24) based on the quadratic penalty (QP) [18] and the successive convex approximation (SCA) [19] methods.

B. Problem Reformulation

In order to deal with the non-convex constraint (24), we first introduce an auxiliary variable $y_{n,m,k}$, such that Constraint (24) can be alternatively written as

$$y_{n,m,k} = x_{m,k} T_{n,k,2}, \quad (26a)$$

$$\sum_{k=1}^{K} T_{n,k,2} \log_2 \left(1 + \frac{\gamma_0 P_{\max} y_{n,m,k}}{T_{n,k,2}(h^2 + \|\mathbf{q}^c_{n,k} - \mathbf{q}_d\|_2^2)} \right) \geq \frac{T_0 R}{B}, \quad (26b)$$

for all $n \in \mathcal{N}, m, k \in \mathcal{K}$. By applying the big-M method [40] to eliminate the bilinear terms, such that Constraint (26a) can be rewritten as

$$(x_{m,k} - 1)M \leq y_{n,m,k} - T_{n,k,2} \leq 0, \quad (27a)$$

$$0 \leq y_{n,m,k} \leq x_{m,k} M, \quad (27b)$$

for all $n \in \mathcal{N}, m, k \in \mathcal{K}$, where M is a large enough constant.

For dealing with (26b), we introduce a non-negative slack variable $\rho_{n,m,k}$ and rewrite (26b) as

$$\sum_{k=1}^{K} T_{n,k,2} \log_2 \left(1 + \frac{\rho_{n,m,k}}{T_{n,k,2}}\right) \geq \frac{T_0 R}{B}, \tag{28a}$$

$$\frac{h^2 + \|\mathbf{q}_{n,k}^{c} - \mathbf{q}_d\|_2^2}{\gamma_0 P_{\max} y_{n,m,k}} \leq \frac{1}{\rho_{n,m,k}}, \tag{28b}$$

for all $n \in \mathcal{N}, m, k \in \mathcal{K}$. Note that $y \log(1 + \frac{x}{y})$ is the perspective of the concave function $\log(1 + x)$, therefore, Constraint (28a) is convex. Meanwhile, it is observed that the left-hand side (LHS) of (28b) is a quadratic-over-linear function, thus (28b) is of the well-known form difference of convex functions. To resolve this issue, we adopt the SCA method to iteratively approximate (28b). Specifically, we take the first-order Taylor term as a tight lower bound of $\frac{1}{\rho_{n,m,k}}$, (28b) is approximated by

$$\frac{h^2 + \|\mathbf{q}_{n,k}^{c} - \mathbf{q}_d\|_2^2}{\gamma_0 P_{\max} y_{n,m,k}} \leq \frac{2}{\bar{\rho}_{n,m,k}} - \frac{\rho_{n,m,k}}{\bar{\rho}_{nmk}^2}, \forall n \in \mathcal{N}, m, k \in \mathcal{K}. \tag{29}$$

Recall that the UAV can only serve one target at a time. The sparsity of the binary indicator vector $\mathbf{x}_k$ can be expressed as $\|\mathbf{x}_k\|_0 \leq 1, \forall k \in \mathcal{K}$. Since the ℓ_0-norm is difficult to handle, we apply the QP technique to solve this issue. Specifically, we first relax $x_{m,k}$ into continuous one, i.e., $x_{m,k} \in [0, 1]$, then we add a quadratic penalty term in the objective function to promote the sparsity of $\mathbf{x}_k$, which is expressed as

$$f = \text{API} - \lambda \sum_{k=1}^{K} \sum_{m=1}^{K} x_{m,k}(x_{m,k} - 1), \tag{30}$$

where $\lambda > 0$ is a large enough penalty coefficient. The quadratic penalty term in (30) is concave. Thus, we can replace it by its first-order Taylor approximation as a tight upper bound, such that

$$f \approx \text{API} - \lambda \sum_{k=1}^{K} \sum_{m=1}^{K} \left((2\bar{x}_{m,k} - 1)x_{m,k} - \bar{x}_{m,k}^2\right), \tag{31}$$

where $\bar{x}_{m,k}$ is the predetermined expansion point. Therefore, Problem (P$_2$) can be approximated by

$$(\text{P}_3) \quad \min_{\substack{\{x_{m,k}, y_{n,m,k}, \rho_{n,m,k}, \\ F_{n,k}, T_{n,k,2}, \mathbf{q}_{n,k}^{s}, \mathbf{q}_{n,k}^{c}\}}} f \tag{32a}$$

$$\text{s.t. } x_{m,k} \in [0, 1], \sum_{m=1}^{K} x_{m,k} = 1, \sum_{k=1}^{K} x_{m,k} = 1,$$

$$(22), (23), (27), (28a), (29), \tag{32b}$$

for all $n \in \mathcal{N}, m, k \in \mathcal{K}$, which is a convex problem and can be solved efficiently through the interior point method.

C. Algorithm Design

To solve Problem (P$_2$), we propose an iterative algorithm by leveraging on the idea of SCA and QP, which is stated in Algorithm 1.

Algorithm 1: Iterative Algorithm for Solving Problem (P$_2$).

Input: $\mathbf{q}_u, \mathbf{q}_v, \mathbf{q}_d, \mathbf{W}, T_0, P_{\max}, N, K, B, h, \phi, v_{\max}, \gamma_0,$
$i = 0, \lambda > 0, \epsilon > 0$.
1: **Initialize** $\bar{x}_{m,k}, \bar{T}_{n,k,2}$ and $\bar{\mathbf{q}}_{n,k}^{c}$ for all n, m, k;
2: **Update** $\bar{y}_{n,m,k} = \bar{x}_{m,k} \bar{T}_{n,k,2}$ and
    $\bar{\rho}_{n,m,k} = \frac{\gamma_0 P_{\max} \bar{y}_{n,m,k}}{h^2 + \|\bar{\mathbf{q}}_{n,k}^{c} - \mathbf{q}_d\|^2}$, for all n, m, k;
3: **repeat**
4: Set $i := i + 1$;
5: Obtain objective value $f^{(i)}$ by solving Problem (P$_3$);
6: Update $\bar{x}_{m,k} = x_{m,k}, \bar{\rho}_{n,m,k} = \rho_{n,m,k}$ for all n, m, k;
7: **until** $\frac{|f^{(i)} - f^{(i-1)}|}{f^{(i-1)}} \leq \epsilon$.
8: **Output:** $\{x_{m,k}, \forall m, k\}$.

---

1) Initialization of Visiting Sequence $\{x_{m,k}, \forall m, k\}$: We propose a heuristic scheme based on the uniform initialization to initialize $x_{m,k}$. Specifically, we set that the first target to visit is the target closest to the UAV starting position $\mathbf{q}_u$, and the last target to visit is the target closest to the first target, so it is convenient to repeat tasks in a new update cycle. Then we set $\bar{x}_{m,k} = \frac{1}{K}, \forall m \in \mathcal{K}, k \in \{2, \cdots, K-1\}$. The purpose of this initialization scheme is to reduce the flight time between adjacent update cycles and ensure that each target is visited fairly within each update cycle.

2) Initialization of Trajectory $\{\mathbf{q}_{n,k}^{s}, \mathbf{q}_{n,k}^{c}, \forall N, K, s\}$: Given the initial visiting sequence, we first give a feasible initialization of trajectory positions which satisfy Problem (P$_3$), i.e.,

$$\bar{\mathbf{q}}_{n,k}^{s} = \mathbf{W} \mathbf{x}_k, \bar{\mathbf{q}}_{n,k}^{c} = \mathbf{q}_d, \forall n \in \mathcal{N}, k \in \mathcal{K}. \tag{33}$$

3) Initialization of Transmission Time $\{T_{n,k,2}, \forall n, k\}$: Inserting $\{\bar{x}_{m,k}, \bar{\mathbf{q}}_{n,k}^{s}, \bar{\mathbf{q}}_{n,k}^{c}\}$ into Problem (P$_2$), we can obtain a feasible initialization of $T_{n,k,2}$. Specifically, we first solve the following linear programming:

$$\{T_{n,k,2}^*\} = \arg \min_{\{T_{n,k,2}\}} \sum_{k=1}^{K} T_{n,k,2} \tag{34a}$$

$$\text{s.t. } \|\bar{\mathbf{q}}_{n,k}^{c} - \bar{\mathbf{q}}_{n,k}^{s}\|_2 \leq v_{\max} T_{n,k,2}, \tag{34b}$$

$$\sum_{k=1}^{K} T_{n,k,2} \log_2 \left(1 + \frac{\gamma_0 P_{\max} \bar{x}_{m,k}}{h^2}\right) \geq \frac{T_0 R}{B}, \tag{34c}$$

for all $n \in \mathcal{N}, k \in \mathcal{K}$. Then we can initialize $\bar{T}_{n,k,2} = T_{n,k,2}^*$.

During the iteration process, the objective function value initially decreases unstable due to the existence of a penalty term in the objective function. It is not until $\{x_{m,k}, \forall m, k\}$ is penalized to a value of 0 or 1 that the objective function decreases steadily. Simulation results show that this algorithm can converge within several iterations. The computational complexity of Algorithm 1 is approximately $\mathcal{O}(I_1(4NK + 2NK^2 + K^2)^3)$ where I_1 represents the number of iterations for achieving convergence. The analysis process of Algorithm 1 is similar to Algorithm 2 in Section V, which is omitted here for brevity.

VI. AVERAGE PAoI MINIMIZATION

Based on the target visiting sequence $\{x_{m,k}, \forall m, k\}$ obtained in the first stage, in this section, we consider Problem (P1) with $S > 1$, i.e., the UAV senses each target multiple times from different views to improve the sensing quality. By replacing $\mathbf{s}_k = \mathbf{W}\mathbf{x}_k, \forall k$, the average PAoI minimization problem is simplified as

$$(\text{P}_4) \quad \min_{\{S, F_{n,k,s}, T_{n,k,2}, \mathbf{q}^{\text{s}}_{n,k,s}, \mathbf{q}^{\text{c}}_{n,k}\}} \text{API} \quad (35a)$$

s.t. (4), (8), (10),

$$\|\mathbf{q}^{\text{s}}_{n,k,s} - \mathbf{s}_k\|_2 \leq r, \quad (35b)$$

$$T_{n,k,2} \log_2\left(1 + \frac{\gamma_0 P_{\max}}{h^2 + \|\mathbf{q}^{\text{c}}_{n,k} - \mathbf{q}_d\|_2^2}\right) \geq \frac{S T_0 R}{B}, \quad (35c)$$

for all $n \in \mathcal{N}, k \in \mathcal{K}, s \in \mathcal{S}$ and $S \in \mathbb{Z}$.

Problem (P4) is a non-convex and mixed-integer programming. However, we observe from (10) the range of values that the integer variable S can take is limited. Thus, we can optimize S by applying the exhaustive method. For a given S, the key challenges of solving Problem (P4) are to deal with non-convex constraints (8), (10), and (35c). By applying the SCA method, we can approximate Problem (P4) with fixed S by a convex problem which can be solved iteratively by off-the-shelf convex solvers, e.g., CVX [41].

A. Problem Analysis

By analyzing the structure of Problem (P4) and the sensing success probability constraint (10), we can obtain the range of the sensing times S. The details of the analysis process are described in Lemma 2.

Lemma 2: The range of the number of sensing is $[S_{\min}, S_{\max}]$, where $S_{\min} = \left\lceil \frac{\log_2(1-P_{\text{th}})}{\log_2(1-e^{-\mu h})} \right\rceil$ and $S_{\max} = \left\lceil \frac{\log_2(1-P_{\text{th}})}{\log_2(1-e^{-\mu\|h^2+r^2\|_2})} \right\rceil$.

Proof: The sensing success probability $p_{n,k,s}$ is a monotonously decreasing function concerning $d_{n,k,s}$. When the UAV hovers directly above the target to perform the sensing task, the maximum sensing success probability for once sensing can be obtained by $p^*_{n,k,s} = e^{-\mu h}$. In this case, we can obtain a lower bound of S, i.e., $S_{\min} = \left\lceil \frac{\log_2(1-P_{\text{th}})}{\log_2(1-p^*_{n,k,s})} \right\rceil$. Due to the existence of $d_{\min}$, all sensing positions can't be directly above the target, thus the lower bound $S_{\min}$ might not be reached. Meanwhile, due to the limited UAV battery capacity and the requirement of the minimum average PAoI, S cannot increase infinitely. Therefore, there must be an upper bound $S_{\max}$ for S. We can get the minimum sensing success probability $p^\star_{n,k,s} = e^{-\mu\|h^2+r^2\|_2}$ under the worst condition, namely, at the edge of the sensing range. Thus, the upper bound of the maximum sensing number is $S_{\max} = \left\lceil \frac{\log_2(1-P_{\text{th}})}{\log_2(1-p^\star_{n,k,s})} \right\rceil$. ∎

To illustrate the range of S, we plot $S_{\min}$ and $S_{\max}$ at different P_{th} for the given parameters ($\mu = 0.05$, $\phi = 45°$, $h = 100$ m) according to Lemma 2. As shown in Fig. 4, S has a finite range of values. Therefore, we can use the exhaustive method (or the
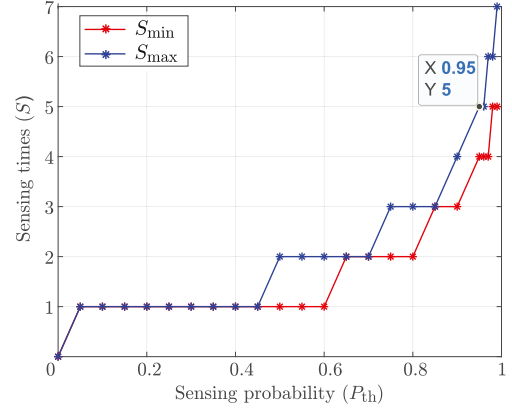

Fig. 4. Number of sensing S vs. the sensing success probability P_{th}.

bisection method) to find the optimal S^* which can minimize the objective function in Problem (35).

B. Problem Reformulation

Follow in the approximate treatment method in [42], the non-convex constraint (8) can be transformed by

$$\|\bar{\mathbf{q}}^{\text{s}}_{n,k,s+1} - \bar{\mathbf{q}}^{\text{s}}_{n,k,s}\|_2 + \bar{L}^T\left(\mathbf{q}^{\text{s}}_{n,k,s+1} - \bar{\mathbf{q}}^{\text{s}}_{n,k,s+1}\right)$$
$$- \bar{L}^T\left(\mathbf{q}^{\text{s}}_{n,k,s} - \bar{\mathbf{q}}^{\text{s}}_{n,k,s}\right) \geq d_{\min}, \forall n \in \mathcal{N}, k \in \mathcal{K}, s \in \bar{\mathcal{S}}, \quad (36)$$

where $\bar{L} = \frac{\bar{\mathbf{q}}^{\text{s}}_{n,k,s+1} - \bar{\mathbf{q}}^{\text{s}}_{n,k,s}}{\|\bar{\mathbf{q}}^{\text{s}}_{n,k,s+1} - \bar{\mathbf{q}}^{\text{s}}_{n,k,s}\|_2}$.

For dealing with Constraint (10), we first take its logarithmic function based on 2, i.e.,

$$\sum_{s=1}^{S} \log_2(1 - e^{-\mu d_{n,k,s}}) \leq \log_2(1 - P_{\text{th}}), \forall n \in \mathcal{N}, k \in \mathcal{K}. \quad (37)$$

Then, we introduce an auxiliary variable $u_{n,k,s}$, such that (37) can be alternatively written as

$$\sum_{s=1}^{S} \log_2(1 - u_{n,k,s}) \leq \log_2(1 - P_{\text{th}}), \quad (38a)$$

$$u_{n,k,s} \leq e^{-\mu d_{n,k,s}}, \quad (38b)$$

for all $n \in \mathcal{N}, k \in \mathcal{K}, s \in \mathcal{S}$. The concave function $\log(1-x)$ can be approximated by its first-order Taylor approximation. Thus, (38a) can be transformed into

$$\sum_{s=1}^{S} \left(\log_2(1 - \bar{u}_{n,k,s}) - \frac{u_{n,k,s} - \bar{u}_{n,k,s}}{(1 - \bar{u}_{n,k,s})\ln 2}\right) \leq \log_2(1 - P_{\text{th}}), \quad (39)$$

for all $n \in \mathcal{N}, k \in \mathcal{K}, s \in \mathcal{S}$, where $\bar{u}_{n,k,s} = e^{-\mu\sqrt{\|\bar{\mathbf{q}}^{\text{s}}_{n,k,s} - \mathbf{s}_k\|_2^2 + h^2}}$. For (38b), we take its logarithmic function based on e and do a simple transformation

$$\ln(u_{n,k,s}) + \mu\sqrt{\|\mathbf{q}^{\text{s}}_{n,k,s} - \mathbf{s}_k\|_2^2 + h^2} \leq 0, \quad (40)$$

for all $n \in \mathcal{N}, k \in \mathcal{K}, s \in \mathcal{S}$. $\ln(u_{n,k,s})$ which is concave can be approximated by an upper bound in (40). Thus, we approximate

Algorithm 2: SCA-based Algorithm for Solving Problem (P$_4$).

Input: $\mathbf{q}_u, \mathbf{q}_v, \mathbf{q}_d, \mathbf{W}, T_0, P_{\max}, N, K, B, h, R, S, P_{\text{th}}, \phi$, $v_{\max}, \gamma_0, \mu, \theta, i = 0, \epsilon > 0$.

1: Initialize $(\mathbf{q}_{n,k,s}^s)^{(0)} = \bar{\mathbf{q}}_{n,k,s}^s, (\mathbf{q}_{n,k}^c)^{(0)} = \bar{\mathbf{q}}_{n,k}^c$, for all n, k, s;

2: Update $\bar{T}_{n,k,2}, \bar{u}_{n,k,s}, \bar{z}_{n,k}$, for all n, k, s;

3: **repeat**

4:     $i := i + 1$;

5:     For given S, obtain $\{F_{n,k,s}^{(i)}, T_{n,k,2}^{(i)}, (\mathbf{q}_{n,k,s}^s)^{(i)}, (\mathbf{q}_{n,k}^c)^{(i)}, \text{API}^{(i)}, \forall n, k, s\}$ by solving Problem (P$_5$);

6:     Update $\bar{\mathbf{q}}_{n,k,s}^s = (\mathbf{q}_{n,k,s}^s)^{(i)}, \bar{u}_{n,k,s} = u_{n,k,s}^{(i)}$, $\bar{z}_{n,k} = z_{n,k}^{(i)}$, for all n, k, s;

7: **until** $\frac{|\text{API}^{(i)} - \text{API}^{(i-1)}|}{\text{API}^{(i-1)}} \leq \epsilon$.

8: **Output:** $\{\text{API}, F_{n,k,s}, T_{n,k,2}, \mathbf{q}_{n,k,s}^s, \mathbf{q}_{n,k}^c, \forall n, k, s\}$.

(40) by

$$\ln(\bar{u}_{n,k,s}) + \frac{\bar{u}_{n,k,s}}{u_{n,k,s}} - 1 + \mu\sqrt{\|\mathbf{q}_{n,k,s}^s - \mathbf{s}_k\|_2^2 + h^2} \leq 0, \tag{41}$$

for all $n \in \mathcal{N}, k \in \mathcal{K}, s \in \mathcal{S}$.

Following the similar procedures to (24) as detailed in Section IV, the reliable transmission constraint (35c) is transformed into

$$T_{n,k,2} B \log_2\left(1 + \frac{z_{n,k}}{T_{n,k,2}}\right) \geq ST_0 R, \forall n \in \mathcal{N}, k \in \mathcal{K}, \tag{42a}$$

$$\frac{h^2 + \|\mathbf{q}_{n,k}^c - \mathbf{q}_d\|_2^2}{T_{n,k,2}\gamma_0 P_{\max}} \leq \frac{2}{\bar{z}_{n,k}} - \frac{z_{n,k}}{\bar{z}_{n,k}^2}, \forall n \in \mathcal{N}, k \in \mathcal{K}, \tag{42b}$$

where $z_{n,k}$ is the introduced auxiliary variable.

By now, Problem (P$_4$) is approximated by a series of convex problems that can be solved iteratively by the existing convex optimization techniques, where

$$(\text{P}_5) \min_{\substack{\{F_{n,k,s}, T_{n,k,2}, \mathbf{q}_{n,k,s}^s, \\ \mathbf{q}_{n,k}^c, u_{n,k,s}, z_{n,k}\}}} \text{API}$$

$$\text{s.t. (4), (35b), (36), (39), (41), (42).} \tag{43}$$

C. Algorithm Design

An iterative algorithm is proposed based on the SCA method to solve Problem (P$_4$). The details are summarized in Algorithm 2. We use the exhaustive method in $[S_{\min}, S_{\max}]$ for acquiring S^* which can minimize the average PAoI.

1) Initialization: We initialize Algorithm 2 by finding a solution that satisfies all constraints of Problem (P$_5$). We first give a series of feasible positions $\{Q_1, Q_2\}$ which can satisfy the UAV trajectory constraints (4a)–(4f), the minimum flight distance constraint (8), the sensing range constraint (35b), as well as reliable transmission constraint (35c), i.e.,

$$Q_1 = \{\bar{\mathbf{q}}_{n,k,s}^s\} = \{(x_k, y_k), (x_k + d_{\min}, y_k),$$

$$(x_k, y_k + d_{\min}), (x_k - d_{\min}, y_k), (x_k, y_k - d_{\min})\}, \tag{44a}$$

$$Q_2 = \bar{\mathbf{q}}_{n,k}^c = \mathbf{q}_d, \tag{44b}$$

for all $n \in \mathcal{N}, k \in \mathcal{K}$. When there are more than five sensing positions $\mathbf{q}_{n,k,s}^s$ to initialize, we can select the positions in Q_1 cyclical. Further, taking the initial feasible trajectory positions into Problem (P$_5$), we can obtain the feasible values of $\{T_{n,k,2}, u_{n,k,s}, z_{n,k}, \forall n, k, s\}$, which are initialized as

$$\bar{u}_{n,k,s} = e^{-\mu\sqrt{\|\bar{\mathbf{q}}_{n,k,s}^s - \mathbf{s}_k\|_2^2 + h^2}}, \tag{45a}$$

$$\bar{T}_{n,k,2} = \max\left\{\frac{ST_0 R}{B\log_2(1 + \frac{\gamma_0 P_{\max}}{h^2})}, \frac{\|\bar{\mathbf{q}}_{n,k,s}^s - \mathbf{q}_d\|_2}{v_{\max}}\right\}, \tag{45b}$$

$$\bar{z}_{n,k} = \frac{\gamma_0 P_{\max} \bar{T}_{n,k,2}}{h^2 + \|\bar{\mathbf{q}}_{n,k}^c - \mathbf{q}_d\|_2^2}, \tag{45c}$$

for all $n \in \mathcal{N}, k \in \mathcal{K}, s \in \mathcal{S}$.

2) Convergence and Complexity Analysis: We focus on the convergence and the complexity analysis of Algorithm 2 in this subsection. The convergence of Algorithm 2 can be guaranteed by Lemma 3.

Lemma 3: When S is fixed, the sequence of the objective value of Problem (P$_4$) is non-increasing with the iteration number i, and it is lower-bounded by zero.

Proof: We define $\text{O}(w^{(i)})$ and $\text{API}(w^{(i)})$ as the objective values of the optimization problems (P$_4$) and (P$_5$), respectively, where $w^{(i)}$ represents the optimal solution at the i-th iteration. The optimization solution obtained at the $(i-1)$-th iteration is set to be the input at the i-th iteration. First, due to the application of the first-order Taylor expansion, the objective function in Problem (P$_4$) is approximated by an upper bound function in Problem (P$_5$), where

$$\text{API}(w|w^{(i)}) \geq \text{O}(w) + c^{(i)}, \tag{46}$$

where $c^{(i)} = \text{API}(w|w^{(i)}) - \text{O}(w)$. Second, the objective of Problem (P$_5$) at the i-th iteration is obtained by the step 3–7 in Algorithm 2, it follows that

$$\text{O}(w^{(i)}) \overset{(a)}{\leq} \text{API}\left(w^{(i)}|w^{(i-1)}\right) - c^{(i-1)} \tag{47a}$$

$$\overset{(b)}{\leq} \text{API}\left(w^{(i-1)}|w^{(i-1)}\right) - c^{(i-1)} = \text{O}\left(w^{(i-1)}\right), \tag{47b}$$

where the inequality (a) follows from (46), and the inequality (b) holds since in step 5 of Algorithm 2, Problem (P$_5$) is solved optimally with solution $w^{(i)}$. Therefore, when S is fixed, the objective value of Problem (P$_4$) is non-increasing with the iteration number i. Moreover, since the objective value is lower bounded by zero, Algorithm 2 can be guaranteed to converge as i goes to infinity [43]. ∎

The total computational complexity of the proposed iterative Algorithm 2 is determined by the number of iterations and the computational complexity for solving Problem (P$_5$) in each iteration [43]. The computational complexity in each iteration

TABLE I
SIMULATION PARAMETERS

Parameters	Values	Parameters	Values
N	5	K	$[1,\cdots,20]$
P_{th}	0.9	$\mathbf{q}_u$	$[0,0]^T$
γ_0	10^6	$\mathbf{q}_d$	$[500,500]^T$
h	100 m	$\mathbf{q}_v$	$[1000,0]^T$
ϵ	10^{-3}	λ	1×10^5
μ	0.005	$\mathbf{W}$	random distribution
B	1 MHz	$P_{\max}$	$[0.01, 0.1, 1.0]$ W
R	1 Mbit/s	T_0	$[0.5, 1.0, 1.5, 2.0]$ s
$v_{\max}$	20 m/s	ϕ	$[15°, 30°, 45°, 60°]$
$T_{\max}$	10^4 s	θ	$[15°, 30°, 45°, 60°]$

is $\mathcal{O}((2NKS + 3NK)^3)$ since there are $2NKS + 3NK$ variables that need to update in each iteration. Therefore, the total computational complexity of Algorithm 2 is $\mathcal{O}(I_2(2NKS + 3NK)^3)$, where I_2 represents the required number of iterations for achieving convergence. Although it is difficult to acquire the exact value of iteration number I_2, multiple simulation results demonstrate that Algorithm 2 converges within dozens of iterations under a given precision. Recall that the exhaustive method is applied to acquire the optimal S^* in the outer loop of Algorithm 2. Therefore, the total algorithm complexity for approximately solving Problem (P4) is $\mathcal{O}(LI_2(2NKS + 3NK)^3)$, where $L = S_{\max} - S_{\min}$.

VII. SIMULATION RESULTS

In this section, numerical results are presented to verify the effectiveness of the proposed algorithm and prove the proposed approach outperforms the benchmark schemes. We consider a network scenario in which the UAV senses K targets distributed randomly in an area with size 1 km × 1 km. For easy setup, we set the packet size of data sensed by the UAV from each target equal. Parameter settings are shown in Table I. Unless stated otherwise, we set $P_{\max} = 1.0$ w, $T_0 = 0.5$ s, $K = 10$, $\theta = 15°$, and $\phi = 45°$.

By solving Problem (P2) with Algorithm 1, we obtain an efficient target visiting sequence (denoted by QP) which can instruct the UAV to complete the sensing and communication services with the freshest information. Furthermore, we introduce two visiting sequence schemes for comparison, i.e.,

- Nearest neighbor visiting policy (NNP): the UAV selects the target closest to its current position to visit every time.
- Random visiting policy (RP): the UAV randomly selects one target to visit every time.

For the benchmark algorithm, the alternating optimal (AO) algorithm [20] is applied to solve Problem (P5). The key idea of the AO algorithm is to optimize the trajectory $\{\mathbf{q}^s_{n,k,s}, \mathbf{q}^c_{n,k}\}$ and service times $\{F_{n,k,s}, T_{n,k,2}\}$ alternately, which reduces into two sub-problems. These two sub-problems are optimized alternately until the algorithm converges.

A. Algorithm Convergence

We provide the relative convergence precision of the proposed algorithm, i.e., $\frac{\text{API}^{(i)} - \text{API}^{(i-1)}}{\text{API}^{(i-1)}}$, during each iteration in Fig. 5.
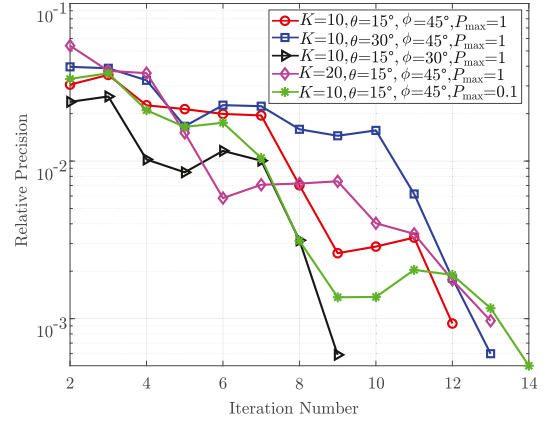

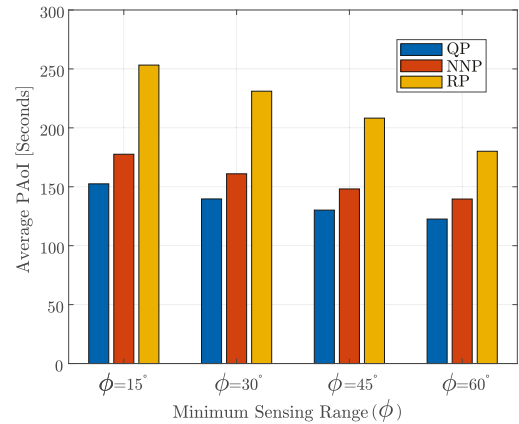Fig. 5.   Relative convergence precision vs. the iteration index.

Fig. 6.   API vs. ϕ under different visiting sequences.

It is observed that the relative convergence accuracy can be guaranteed to be lower than 10^{-3} within several iterations for different parameters, i.e., K, θ, ϕ, and $P_{\max}$. This indicates that the proposed algorithm can converge quickly under different parameter settings.

B. Visiting Sequence Comparison

In this subsection, we first evaluate the impact of the different target visiting sequences on the average PAoI under different parameter settings. Then, we study the impact of target spatial distribution on the algorithm performance.

The impact of different visiting sequences on the average PAoI, referred to as API, under different values of ϕ, θ, and T_0 is shown in Figs. 6–8. The proposed QP has the best performance compared with RP and NNP, which is always true for different parameters ϕ, θ, and T_0. As shown in Figs. 6–8, it is observed that RP without optimizing the visiting sequence has the worst performance, and the performance of NNP is between QP and RP. This is because each selection of the NNP is the shortest distance. In scenarios where the targets are distributed sparsely, the shortest path of each step may not mean the overall shortest trajectory. Moreover, it is observed in Fig. 6 that API decreases with the increase of ϕ. When the sensing range ϕ becomes larger, the distance between the UAV and the targets can be larger for performing sensing, which potentially saves the UAV flight time.
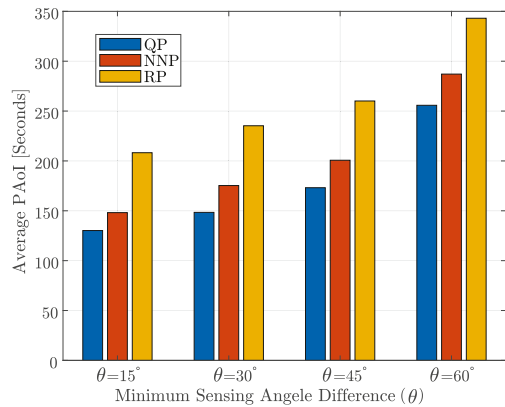
Fig. 7. API vs. θ under different visiting sequences.
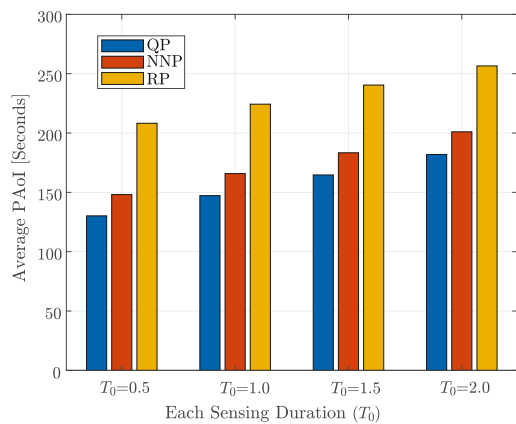
Fig. 8. API vs. T_0 under different visiting sequences.

Fig. 9. Optimized UAV trajectories with $K = 10$, $\theta = 30°$ under QP and NNP in two different target spatial distribution scenarios. In scenarios 1 and 2, $K = 10$ targets are randomly scattered in an area of 1 km × 1 km. (a) QP for scenario 1, objective function value API = 148.6138 s. (b) NNP for scenario 1, objective function value API = 155.6164 s. (c) QP for scenario 2, objective function value API = 148.4143 s. (d) NNP for scenario 2, objective function value API = 175.3169 s.

It is observed in Fig. 7 that API increases with the increase of θ. However, when the view angle difference θ becomes larger, the UAV needs to fly a longer distance to adjust the sensing positions. The increase in sensing time T_0 also results in an increase in API, which is shown in Fig. 8. In conclusion, optimizing the target visiting sequence is critical to improving the information freshness.

The impact of the target spatial distribution on the optimal UAV trajectory is shown in Fig. 9, where the UAV trajectory in the first update cycle is shown. First, it is observed that the optimized UAV trajectories in different target spatial distribution scenarios are different by comparing Fig. 9(a) and (c). Second, the proposed QP always has lower API than NNP which is based on the greedy strategy. This is because NNP selects the target to be sensed according to the policy of the shortest path of each step while QP tries to find the global optimal trajectory when determining the target visiting sequence. Note that the performance gap between QP and NNP can vary depending on the target spatial distribution. Specifically, by comparing Fig. 9(a) and (b), Fig. 9(c) and (d), the performance gaps between QP and NNP in scenarios 1 and 2 are 7.0026 s and 26.9026 s, respectively. Although the performance improvement of QP relative to NNP is limited in scenario 1 where the target distribution is simple, QP always has better performance than NNP, especially in scenarios where targets are not distributed evenly.
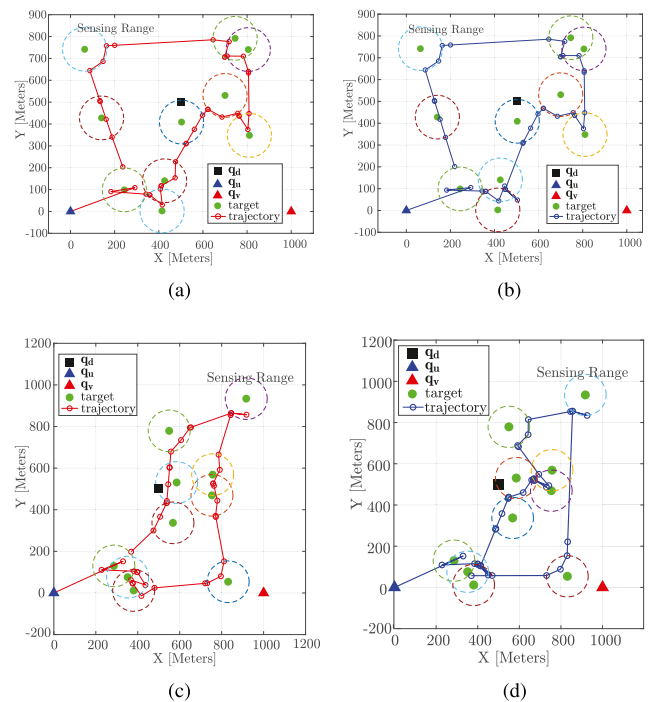
C. Trajectory Optimization

In this subsection, we present the optimized UAV trajectories under different parameters P_{max}, ϕ, and θ. To be clear, the impact of the parameter settings on the optimized trajectories is similar in different target distribution scenarios. Thus, we only present the optimized UAV trajectory in scenario 1.

The impact of the transmit power P_{max} on the UAV trajectory is shown in Fig. 10(a). It is observed that the transmission end positions of the UAV tend to be close to the GC when its transmit power P_{max} is small, e.g., 0.01 W in our simulation. This is because after performing the sensing task for one target, the UAV tends to move closer to the GC for improving the communication quality so that the transmit time will be reduced, especially when the UAV transmit power is low. Nonetheless, the movement of the UAV will cause an increase in flight time thereby limiting the performance improvement in average PAoI, which is also verified in Fig. 12. Improving the communication quality by enlarging P_{max} can save transmission time, but at the cost of increasing flight time, which indicates that we need to weigh whether it is worth it to trade more power consumption for limited performance gains in practical applications.

In Fig. 10(b), the impact of the UAV maximum sensing angle ϕ on the optimized trajectory is presented. A large value of ϕ means a large sensing range of the sensors equipped in the UAV. As long as the targets are within the sensing range of the onboard
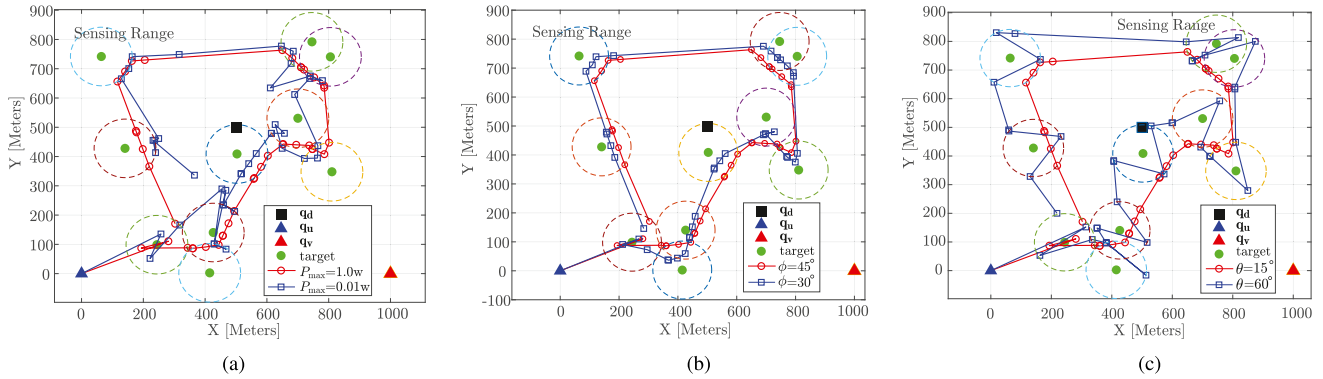
Fig. 10.   Comparisons of the optimized UAV trajectories under different parameter settings in scenario 1. (a) Optimized trajectory vs. $P_{\max}$. (b) Optimized trajectory vs. ϕ. (c) Optimized trajectory vs. θ.
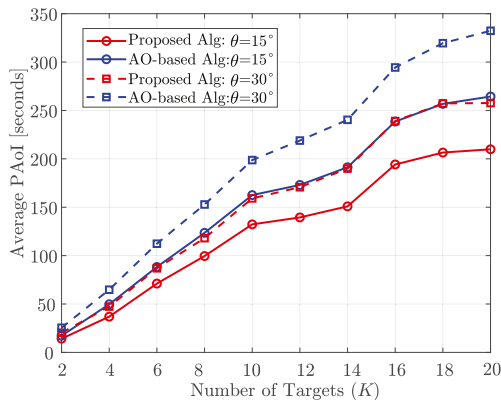

Fig. 11.   API vs. K under the different values of θ.
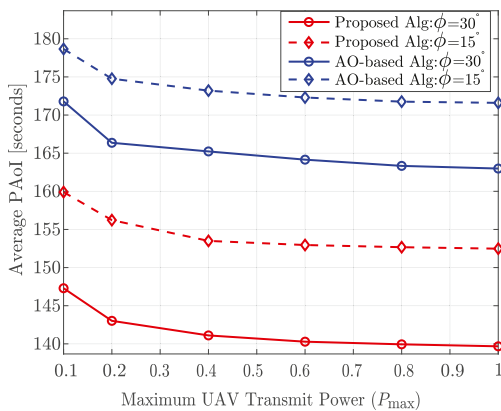

Fig. 12.   API vs. ϕ under the different values of $P_{\max}$.

sensor, the UAV tends to be far away from targets for reducing the flight time, API will thus decrease, as shown in Fig. 12.

The impact of the view angle difference θ on the UAV trajectory is shown in Fig. 10(c). When θ increases, the UAV trajectory will have more folds for sensing information from different views. This is because the distance between adjacent sensing positions will increase to ensure that it is no less than $d_{\min}$. A large value of θ will cause an increase in API, which is also proved in Figs. 7 and 11. To sum up, improving the sensing

quality comes at the cost of increasing flight time, which leads to an increase in average PAoI. Therefore, we should carefully balance the information freshness and the sensing quality when implementing the actual system design.

D. Algorithm Comparison

In this subsection, we compare the performance of the proposed algorithm with the AO algorithm under different parameters K, θ, ϕ, and $P_{\max}$.

As shown in Fig. 11, the average PAoI increases with the number of targets K. A large K means that the service time for the UAV to complete an update cycle is long, thus leading to an increase in the average PAoI. Since targets are randomly distributed in our considered scenario, the average PAoI increases irregularly. Meanwhile, the view angle difference θ also has an obvious impact on the objective function, e.g., API grows when θ changes from $15°$ to $30°$. As presented in Figs. 7 and 10(c), increasing θ means that $d_{\min}$ becomes larger, which leads to an increase in the UAV flight time between adjacent sensing positions. Furthermore, the proposed algorithm outperforms the AO algorithm under the same values of K and θ. When K increases, the objective function of the proposed algorithm increases slower than that of the AO algorithm.

As shown in Fig. 12, the average PAoI gradually decreases with the UAV transmit power $P_{\max}$ increasing. This is because increasing $P_{\max}$ can provide a better communication quality and reduce transmission time, which has been stated in Fig. 10(a). We also observe that the average PAoI when $\phi = 30°$ is smaller than that when $\phi = 15°$. The impact of ϕ on the objective function has been proved in Figs. 6 and 10(b). Furthermore, the proposed algorithm performs better than the AO algorithm. It is observed that the average PAoI of the proposed algorithm is always smaller than that of the AO algorithm for the same values of ϕ and $P_{\max}$. The average PAoI of the proposed algorithm decreases faster than that of the AO algorithm with $P_{\max}$ increasing.

VIII. Conclusion

In this article, we have developed a *MUSIC* framework for a UAV-based wireless sensing and communication scenario with

known target positions. To improve the freshness of information received at the GC, we have investigated an average PAoI minimization problem by jointly optimizing the parameters contained in this framework. Then, we have proposed a two-stage approach based on the QP, SCA, and exhaustive methods to solve the formulated problem for obtaining a sub-optimal solution. The proposed approach can be applied to support UAV-based sensing applications that require sensing precision, communication quality, and freshness of information. For future work, we will consider the cooperation of multiple UAVs for AoI optimization in time-critical applications.

REFERENCES

[1] G. Geraci et al., "What will the future of UAV cellular communications be? A flight from 5G to 6G," *IEEE Commun. Surv. Tuts.*, vol. 24, no. 3, pp. 1304–1335, thirdquarter 2022.

[2] Y. Zeng, Q. Wu, and R. Zhang, "Accessing from the sky: A tutorial on UAV communications for 5G and beyond," *Proc. IEEE*, vol. 107, no. 12, pp. 2327–2375, Dec. 2019.

[3] Z. Ma, B. Ai, R. He, Z. Zhong, and M. Yang, "A non-stationary geometry-based MIMO channel model for millimeter-wave UAV networks," *IEEE J. Sel. Area Commun.*, vol. 39, no. 10, pp. 2960–2974, Oct. 2021.

[4] M. Vaezi et al., "Cellular, wide-area, and non-terrestrial IoT: A survey on 5G advances and the road towards 6G," *IEEE Commun. Surv. Tuts.*, vol. 24, no. 2, pp. 1117–1174, Secondquarter 2022.

[5] Y. Li et al., "Unmanned aerial vehicle remote sensing for Antarctic research: A review of progress, current applications, and future use cases," *IEEE Geosci. Remote Sens. Mag.*, vol. 11, no. 1, pp. 73–93, Mar. 2023.

[6] H. Zhang, L. Song, and Z. Han, *Unmanned Aerial Vehicle Applications Over Cellular Networks for 5G and Beyond*. Cham, Switzerland: Springer, 2020.

[7] M. Li, J. Gao, L. Zhao, and X. Shen, "Adaptive computing scheduling for edge-assisted autonomous driving," *IEEE Trans. Veh. Technol.*, vol. 70, no. 6, pp. 5318–5331, Jun. 2021.

[8] F. Outay, H. A. Mengash, and M. Adnan, "Applications of unmanned aerial vehicle (UAV) in road safety, traffic and highway infrastructure management: Recent advances and challenges," *Transp. Res. Part A: Policy Pract.*, vol. 141, pp. 116–129, 2020.

[9] A. Sharma and P. K. Singh, "UAV-based framework for effective data analysis of forest fire detection using 5G networks: An effective approach towards smart cities solutions," *Int. J. Commun. Syst.*, 2021, Art. no. e4826.

[10] S. M. S. M. Daud et al., "Applications of drone in disaster management: A scoping review," *Sci. Justice*, vol. 62, no. 1, pp. 30–42, 2022.

[11] G. Messina and G. Modica, "Applications of UAV thermal imagery in precision agriculture: State of the art and future research outlook," *Remote Sens.*, vol. 12, no. 9, 2020, Art. no. 1491.

[12] S. Feroz and S. A. Dabous, "UAV-based remote sensing applications for bridge condition assessment," *Remote Sens.*, vol. 13, no. 9, 2021, Art. no. 1809.

[13] M. Li, C. Chen, H. Wu, X. Guan, and X. Shen, "Age-of-information aware scheduling for edge-assisted industrial wireless networks," *IEEE Trans. Ind. Informat.*, vol. 17, no. 8, pp. 5562–5571, Aug. 2021.

[14] S. Kaul, R. Yates, and M. Gruteser, "Real-time status: How often should one update?," in *Proc. IEEE INFOCOM*, 2012, pp. 2731–2735.

[15] M. A. Abd-Elmagid, N. Pappas, and H. S. Dhillon, "On the role of Age of Information in the Internet of Things," *IEEE Commun. Mag.*, vol. 57, no. 12, pp. 72–77, Dec. 2019.

[16] A. Kosta, N. Pappas, and V. Angelakis, "Age of Information: A new concept, metric, and tool," *Found. Trends Netw.*, vol. 12, no. 3, pp. 162–259, 2017.

[17] R. D. Yates, Y. Sun, D. R. Brown, S. K. Kaul, E. Modiano, and S. Ulukus, "Age of Information: An introduction and survey," *IEEE J. Sel. Areas Commun.*, vol. 39, no. 5, pp. 1183–1210, May 2021.

[18] D. P. Bertsekas, "On penalty and multiplier methods for constrained minimization," *Nonlinear Program.*, vol. 14, no. 2, pp. 165–191, 1975.

[19] W. Li, T. Chang, and C. Chi, "Multicell coordinated beamforming with rate outage constraint—Part II: Efficient approximation algorithms," *IEEE Trans. Signal Process.*, vol. 63, no. 11, pp. 2763–2778, Jun. 2015.

[20] Q. Wu, Y. Zeng, and R. Zhang, "Joint trajectory and communication design for multi-UAV enabled wireless networks," *IEEE Trans. Wireless Commun.*, vol. 17, no. 3, pp. 2109–2121, Mar. 2018.

[21] J. Gong, T. Chang, C. Shen, and X. Chen, "Flight time minimization of UAV for data collection over wireless sensor networks," *IEEE J. Sel. Area Commun.*, vol. 36, no. 9, pp. 1942–1954, Sep. 2018.

[22] C. Zhan and Y. Zeng, "Completion time minimization for multi-UAV-enabled data collection," *IEEE Trans. Wireless Commun.*, vol. 18, no. 10, pp. 4859–4872, Oct. 2019.

[23] X. Zhang and L. Duan, "Energy-saving deployment algorithms of UAV swarm for sustainable wireless coverage," *IEEE Trans. Veh. Technol.*, vol. 69, no. 9, pp. 10320–10335, Sep. 2020.

[24] R. Ding, F. Gao, and X. S. Shen, "3D UAV trajectory design and frequency band allocation for energy-efficient and fair communication: A deep reinforcement learning approach," *IEEE Trans. Wireless Commun.*, vol. 19, no. 12, pp. 7796–7809, Dec. 2020.

[25] M. Li, N. Cheng, J. Gao, Y. Wang, L. Zhao, and X. Shen, "Energy-efficient UAV-assisted mobile edge computing: Resource allocation and trajectory optimization," *IEEE Trans. Veh. Technol.*, vol. 69, no. 3, pp. 3424–3438, Mar. 2020.

[26] K. Wang, X. Zhang, L. Duan, and J. Tie, "Multi-UAV cooperative trajectory for servicing dynamic demands and charging battery," *IEEE Trans. Mobile Comput.*, vol. 22, no. 3, pp. 1599–1614, Mar. 2023.

[27] W. Jiang, C. Shen, B. Ai, and H. Li, "Peak age of information minimization for UAV-aided wireless sensing and communications," in *Proc. IEEE Int. Conf. Commun. Workshops*, 2021, pp. 1–6.

[28] M. A. Abd-Elmagid and H. S. Dhillon, "Average peak age-of-information minimization in UAV-assisted IoT networks," *IEEE Trans. Veh. Technol.*, vol. 68, no. 2, pp. 2003–2008, Feb. 2019.

[29] C. Zhou et al., "Deep RL-based trajectory planning for AoI minimization in UAV-assisted IoT," in *Proc. 11th Int. Conf. Wireless Commun. Signal Process.*, 2019, pp. 1–6.

[30] K. Liu and J. Zheng, "UAV trajectory optimization for time-constrained data collection in UAV-enabled environmental monitoring systems," *IEEE Internet Things J.*, vol. 9, no. 23, pp. 24300–24314, Dec. 2022.

[31] S. Zhang, H. Zhang, B. Di, and L. Song, "Joint trajectory and power optimization for UAV sensing over cellular networks," *IEEE Commun. Lett.*, vol. 22, no. 11, pp. 2382–2385, Nov. 2018.

[32] S. Zhang, H. Zhang, Z. Han, H. V. Poor, and L. Song, "Age of Information in a cellular Internet of UAVs: Sensing and communication trade-off design," *IEEE Trans. Wireless Commun.*, vol. 19, no. 10, pp. 6578–6592, Oct. 2020.

[33] J. Hu, H. Zhang, L. Song, R. Schober, and H. V. Poor, "Cooperative internet of UAVs: Distributed trajectory design by multi-agent deep reinforcement learning," *IEEE Trans. Commun.*, vol. 68, no. 11, pp. 6807–6821, Nov. 2020.

[34] F. Wu, H. Zhang, J. Wu, Z. Han, H. V. Poor, and L. Song, "UAV-to-device underlay communications: Age of Information minimization by multi-agent deep reinforcement learning," *IEEE Trans. Commun.*, vol. 69, no. 7, pp. 4461–4475, Jul. 2021.

[35] F. Liu et al., "Integrated sensing and communications: Towards dual-functional wireless networks for 6G and beyond," *IEEE J. Sel. Areas Commun.*, vol. 40, no. 6, pp. 1728–1767, Jun. 2022.

[36] F. Peng, Z. Jiang, S. Zhou, Z. Niu, and S. Zhang, "Sensing and communication co-design for status update in multiaccess wireless networks," *IEEE Trans. Mobile Comput.*, vol. 22, no. 3, pp. 1779–1792, Mar. 2023.

[37] V. V. Shakhov and I. Koo, "Experiment design for parameter estimation in probabilistic sensing models," *IEEE Sensors J.*, vol. 17, no. 24, pp. 8431–8437, Dec. 2017.

[38] A. Hossain, P. K. Biswas, and S. Chakrabarti, "Sensing models and its impact on network coverage in wireless sensor network," in *Proc. IEEE Region 10 Third Int. Conf. Ind. Inf. Syst.*, 2008, pp. 1–5.

[39] G. T. 36.777, "Enhanced LTE support for aerial vehicles," 2018. [Online]. Available: http://www.3gpp.org/ftp/Specs/archive/36series/36.777

[40] M. Cococcioni and L. Fiaschi, "The big-M method with the numerical infinite M," *Optim. Lett.*, vol. 15, pp. 2455–2468, 2020.

[41] M. Grant and S. Boyd, "CVX: Matlab software for disciplined convex programming, version 2.1," Mar. 2014. [Online]. Available: http://cvxr.com/cvx

[42] C. Shen, T. Chang, J. Gong, Y. Zeng, and R. Zhang, "Multi-UAV interference coordination via joint trajectory and power control," *IEEE Trans. Signal Process.*, vol. 68, pp. 843–858, 2020.

[43] S. Boyd and L. Vandenberghe, *Convex Optimization*. Cambridge, U.K.: Cambridge Univ. Press Mar. 2004.

Wenwen Jiang (Graduate Student Member, IEEE) received the B.S. degree in communication engineering from Shandong Normal University, Jinan, China, in 2018. She is currently working toward the Ph.D. degree with the State Key Laboratory of Rail Traffic Control and Safety, Beijing Jiaotong University, Beijing, China. From 2022 to 2023, she was a Visiting Ph.D. Student with BBCR Group, Department of Electrical and Computer Engineering, University of Waterloo, Waterloo, ON, Canada. Her research interests include UAV communications, age of information (AoI), IRS-assisted communications, and mobile edge computing.

Bo Ai (Fellow, IEEE) received the M.S. and Ph.D. degrees from Xidian University, Xi'an, China, in 2002 and 2004, respectively. He was with Tsinghua University, Beijing, China, where he was an Excellent Postdoctoral Research Fellow in 2007. He was a Visiting Professor with the Electrical Engineering Department, Stanford University, Stanford, CA, USA, in 2015. He is currently a Full Professor with Beijing Jiaotong University, where he is the Dean of the School of Electronic and Information Engineering, Deputy Director of the State Key Laboratory of Rail Traffic Control and Safety, and the Deputy Director of the International Joint Research Center. He is one of the directors of the Beijing Urban Rail Operation Control System International Science and Technology Cooperation Base, and the Backbone Member of the Innovative Engineering based jointly granted by the Chinese Ministry of Education and the State Administration of Foreign Experts Affairs. He is the research team Leader of 26 national projects. He holds 26 invention patents. He has authored or coauthored eight books and authored more than 300 academic research articles in his research, which include research and applications of channel measurement, channel modeling, and dedicated mobile communications for rail traffic systems. Five papers have been the ESI highly cited paper. He has won some important scientific research prizes. He has been notified by the Council of Canadian Academies that based on the Scopus database, he has been listed as one of the top 1% authors in his field all over the world. He has also been feature-interviewed by the IET Electronics Letters. Dr. Ai is a Fellow of Institution of Engineering and Technology (IET), and IEEE VTS Distinguished Lecturer. He is the recipient of the Distinguished Youth Foundation and Excellent Youth Foundation from the National Natural Science Foundation of China, Qiushi Outstanding Youth Award by the Hong Kong Qiushi Foundation, New Century Talents by the Chinese Ministry of Education, Zhan Tianyou Railway Science and Technology Award by the Chinese Ministry of Railways, and Science and Technology New Star by the Beijing Municipal Science and Technology Commission. He is the IEEE VTS Beijing Chapter Vice Chair and IEEE BTS Xi'an Chapter Chair. He was the co-chair or a session/track chair of many international conferences. He is an Associate Editor for the IEEE ANTENNAS AND WIRELESS PROPAGATION LETTERS and the IEEE TRANSACTIONS ON CONSUMER ELECTRONICS, and an Editorial Committee Member of the *Wireless Personal Communications Journal*. He is the Lead Guest Editor of Special Issues on the IEEE TRANSACTIONS ON VEHICULAR TECHNOLOGY, the IEEE ANTENNAS AND PROPAGATIONS LETTERS, and the INTERNATIONAL JOURNAL ON ANTENNAS AND PROPAGATIONS.

Chao Shen (Member, IEEE) received the B.S. degree in communication engineering and the Ph.D. degree in signal and information processing from Beijing Jiaotong University (BJTU), Beijing, China, in 2003 and 2012, respectively. He was a Visiting Scholar with the University of Maryland at College Park, College Park, MD, USA, from 2014 to 2015, and The Chinese University of Hong Kong, Shenzhen, China, from 2017 to 2018. Since 2012, he has been an Associate Professor with the State Key Laboratory of Rail Traffic Control and Safety, BJTU. Since 2022, he has been a Senior Research Scientist with Shenzhen Research Institute of Big Data, Shenzhen. His research interests include large-scale network optimization, ultrareli1122 able and low-latency communication (URLLC), and integrated sensing and communication (ISAC) for B5G/6G communications.

Mushu Li (Member, IEEE) received the M.A.Sc. degree from Toronto Metropolitan University, Toronto, ON, Canada, in 2017, and the Ph.D. degree in electrical and computer engineering from the University of Waterloo, Waterloo, ON, Canada, in 2021. She is currently a Postdoctoral Fellow with Toronto Metropolitan University. From 2021 to 2022, she was a Postdoctoral Fellow with the University of Waterloo, Waterloo, ON, Canada. Her research interests include mobile edge computing, the system optimization in wireless networks, and machine learning-assisted network management. She was the recipient of Natural Science and Engineering Research Council of Canada (NSERC) Postdoctoral Fellowship in 2022, NSERC Canada Graduate Scholarship in 2018, and Ontario Graduate Scholarship between 2015 and 2016.

Xuemin (Sherman) Shen (Fellow, IEEE) received the Ph.D. degree in electrical engineering from Rutgers University, New Brunswick, NJ, USA, in 1990. He is currently a University Professor with the Department of Electrical and Computer Engineering, University of Waterloo, Waterloo, ON, Canada. His research interests include network resource management, wireless network security, Internet of Things, 5G and beyond, and vehicular networks. Dr. Shen is a registered Professional Engineer of Ontario, Canada, Engineering Institute of Canada Fellow, Canadian Academy of Engineering Fellow, Royal Society of Canada Fellow, Chinese Academy of Engineering Foreign Member, and Distinguished Lecturer of the IEEE Vehicular Technology Society and Communications Society. Dr. Shen was the recipient of the Canadian Award for Telecommunications Research from the Canadian Society of Information Theory (CSIT) in 2021, R.A. Fessenden Award in 2019 from IEEE, Canada, Award of Merit from the Federation of Chinese Canadian Professionals (Ontario) in 2019, James Evans Avant Garde Award in 2018 from the IEEE Vehicular Technology Society, Joseph LoCicero Award in 2015 and Education Award in 2017 from the IEEE Communications Society, and Technical Recognition Award from Wireless Communications Technical Committee in 2019, and AHSN Technical Committee in 2013. He was also the recipient of the Excellent Graduate Supervision Award in 2006 from the University of Waterloo and the Premier's Research Excellence Award (PREA) in 2003 from the Province of Ontario, Canada. He was the Technical Program Committee Chair/Co-Chair for IEEE Globecom' 16, IEEE Infocom'14, IEEE VTC'10 Fall, IEEE Globecom'07, and the Chair for the IEEE Communications Society Technical Committee on Wireless Communications. Dr. Shen was the President of the IEEE Communications Society. He was the Vice President for Technical & Educational Activities, Vice President for Publications, Member-at-Large on the Board of Governors. He was/is the Editor-in-Chief of IEEE INTERNET OF THINGS JOURNAL, IEEE NETWORK, *IET Communications*, and *Peer-to-Peer Networking and Applications*.